

# New Measurements of $V_{cb}$ at CLEO

David H Miller\* †

Physics Department, Purdue University, West Lafayette, IN 47906 USA

E-mail: miller@physics.purdue.edu

ABSTRACT: This paper presents two new results on the measurement of  $V_{cb}$ .

## 1. Introduction

Precision measurements of the elements of the CKM quark matrix are important in understanding the standard model and searching for physics beyond the standard model. Two new results are presented in this paper on the measurement of  $V_{cb}$ . A more detailed description of these results and the eventual published papers will be found at <http://www.lns.cornell.edu/public/CLNS/CLEO.html>.

## 2. Determination of $V_{cb}$ from $B \rightarrow D^* \ell \nu$ decays.

This analysis involves using standard techniques to select decays with a  $D^*$  and a lepton. For each candidate selected the following is computed.

$$\cos \theta_{B-D^* \ell} = \frac{2E_B E_{D^* \ell} - m_B^2 - m_{D^* \ell}^2}{2|\mathbf{p}_B||\mathbf{p}_{D^* \ell}|}. \quad (2.1)$$

This quantity helps distinguish signal from  $D^* X \ell \nu$  background and bounds the flight direction of the  $B$  relative to the  $D^*$ , which is needed to calculate  $w$ , where  $w = v_B \cdot v_{D^*}$  is the relativistic boost  $\gamma$  of the  $D^*$  in the  $B$  rest frame.

In order to disentangle the  $D^* \ell \nu$  from the  $D^* X \ell \nu$  decays, a binned maximum likelihood is used to the  $\cos \theta_{B-D^* \ell}$  distribution. A typical fit is shown in Figure 1. In this fit, the normalizations of the various background distributions are fixed, and those for  $D^* \ell \nu$  and  $D^* X \ell \nu$  float. Given the measured  $D^* \ell \nu$  yields in ten bins of  $w$ , a fit is performed to extract the partial rate,

$$\frac{d\Gamma}{dw} = \frac{G_F^2}{48\pi^3} \mathcal{K}(w) [|V_{cb}| \mathcal{F}(w)]^2, \quad (2.2)$$

\*Speaker.

†On behalf of the CLEO collaboration.

where  $\mathcal{K}(w)$  is a known function of kinematic variables and  $\mathcal{F}(w)$  is the form factor. For the fit a form factor parameterization is used [2] with HQET and dispersion relation constraints [3]. This depends on the form factor ratios  $R_1$  and  $R_2$ , which are taken from a previous measurement [4] in agreement with theoretical expectations [5]. The slope  $\rho^2$  of the form factor at  $w = 1$  is the only shape parameter and it is allowed to vary in the fit.

The  $D^*\ell\nu$  yields are fitted as a function of  $w$  for  $\mathcal{F}(1)|V_{cb}|$  and  $\rho^2$ , keeping  $R_1$  and  $R_2$  fixed at their measured values. The result of the fit is shown in Figure 2. The results are

$$|V_{cb}|F(1) = 0.0422 \pm 0.0013 \pm 0.0018, \quad (2.3)$$

$$\rho^2 = 1.61 \pm 0.09 \pm 0.21, \quad \text{and} \quad (2.4)$$

$$f_{+-} = 0.523 \pm 0.012 \quad (2.5)$$

with a correlation coefficient between  $|V_{cb}|F(1)$  and  $\rho^2$  of 0.86. Integrated over  $w$  these parameters give  $\Gamma = 0.0376 \pm 0.0012 \pm 0.0024 \text{ ps}^{-1}$ , implying branching fractions  $\mathcal{B}(\bar{B}^0 \rightarrow D^{*+}\ell^-\bar{\nu}) = 5.82\%$  and  $\mathcal{B}(B^- \rightarrow D^{*0}\ell^-\bar{\nu}) = 6.21\%$ . Our result for  $\mathcal{F}(1)|V_{cb}|$  gives

$$|V_{cb}| = 0.0462 \pm 0.0014(\text{stat.}) \pm 0.0020(\text{syst.}) \pm 0.0021(\text{theor.}) \quad (2.6)$$

where  $\mathcal{F}(1) = 0.913 \pm 0.042$  is used as input.

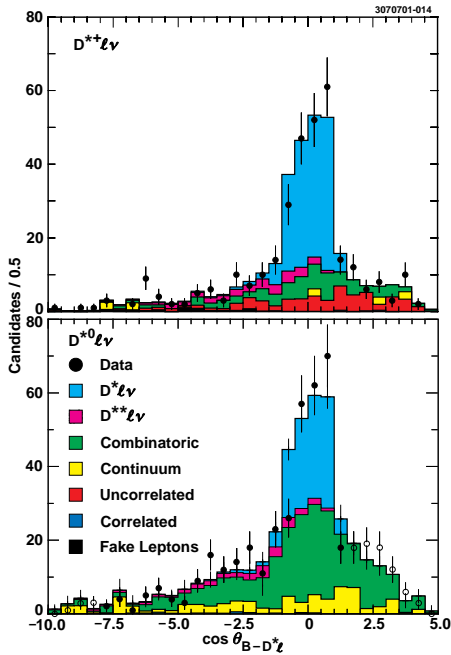


**Figure 1:** The event yields in a typical  $w$  bin with the results of the fit superimposed.

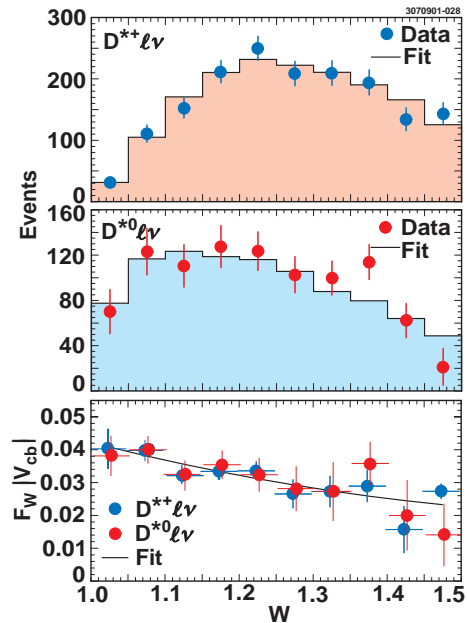


**Figure 2:** The results of the fit to the  $w$  distribution. The bottom figure displays  $|V_{cb}|F(w)$ .

### 3. Analysis of the decay $b \rightarrow s\gamma$

The  $b \rightarrow s\gamma$  decay gives a roughly monoenergetic photon, with  $E_\gamma \approx m_b/2 \approx 2.3 \text{ GeV}$ . In this analysis the spectrum down to 2.0 GeV is used, which includes  $\sim 90\%$  of the  $b \rightarrow s\gamma$

yield. Figure 3 shows the photon spectrum. The fully subtracted spectrum, On - Off - other  $B$  decay processes, is shown in Figure 4. The region of interest for  $b \rightarrow s\gamma$  is 2.0 - 2.8 GeV.

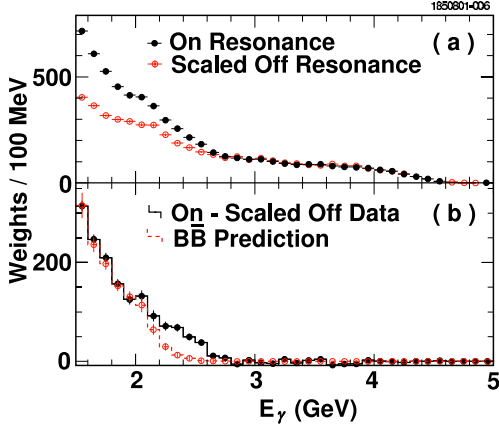


**Figure 3:** Photon energy spectra (weights per 100 MeV). The upper plot (a) shows the On  $\Upsilon(4S)$  and scaled Off-resonance spectra. The lower plot (b) shows their difference.

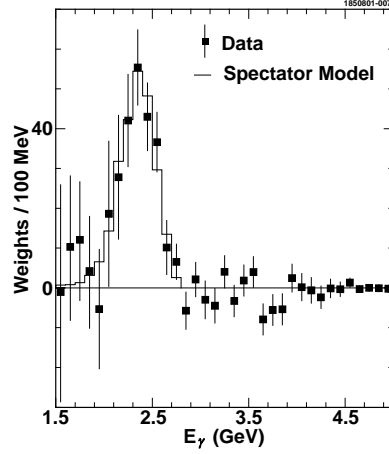


**Figure 4:** Photon energy spectrum for On minus scaled Off minus  $B$  backgrounds. (Also shown is the Ali-Greub spectator model.)

The  $b \rightarrow s\gamma$  branching fraction is obtained by taking the yield between 2.0 and 2.7 GeV,  $233.6 \pm 31.2 \pm 13.4$  weights. The efficiency is  $(3.93 \pm 0.15 \pm 0.17) \times 10^{-2}$  weights per event. This yields an uncorrected branching ratio of  $(3.06 \pm 0.41 \pm 0.26) \times 10^{-4}$ .

The branching fraction is corrected down by  $(4.0 \pm 1.6)\%$ , to remove the  $b \rightarrow d\gamma$  contribution. The fraction of  $b \rightarrow s\gamma$  decays with photon energies above 2.0 GeV is sensitive to the  $b$  mass and Fermi momentum. The fraction  $0.915^{+0.027}_{-0.055}$ , as given by Neubert[6, 9] is used to extrapolate the branching fraction to the full energy range (actually, to energies above 0.25 GeV). With these two corrections the result is

$$\mathcal{B}(b \rightarrow s\gamma) = (3.21 \pm 0.43 \pm 0.27^{+0.18}_{-0.10}) \times 10^{-4} ,$$

for the branching fraction for  $b \rightarrow s\gamma$  alone, over all energies. This result is in good agreement with the Standard Model prediction.

The first and second moments of the photon energy spectrum have been calculated, and the moments in the  $B$  rest frame, for  $E_\gamma(\text{restframe}) > 2.0$  GeV are:

$$\langle E_\gamma \rangle = 2.346 \pm 0.032 \pm 0.011 \text{ GeV} .$$

$$\langle E_\gamma^2 \rangle - \langle E_\gamma \rangle^2 = 0.0226 \pm 0.0066 \pm 0.0020 \text{ GeV}^2 .$$

The expressions [7],[8] for the moments of the photon energy spectrum in  $B \rightarrow X_s\gamma$ , for  $E_\gamma > 2.0$  GeV, in the  $\overline{MS}$  scheme, to order  $\beta_0\alpha_s^2$  and  $1/M_B^3$ , are given in Eqs. 3.1 and 3.2.

$$\begin{aligned} \langle E_\gamma \rangle = & \frac{M_B}{2} [1 - .385 \frac{\alpha_s}{\pi} - .620 \beta_0 (\frac{\alpha_s}{\pi})^2 - \frac{\bar{\Lambda}}{M_B} (1 - .954 \frac{\alpha_s}{\pi} - 1.175 \beta_0 (\frac{\alpha_s}{\pi})^2)] \\ & - \frac{13\rho_1 - 33\rho_2}{24M_B^2} - \frac{\mathcal{T}_1 + 3\mathcal{T}_2 + \mathcal{T}_3 + 3\mathcal{T}_4}{8M_B^2} - \frac{\rho_2 C_2}{18M_D^2 C_7} + \mathcal{O}(1/M_B^3). \end{aligned} \quad (3.1)$$

$$\begin{aligned} \langle (E_\gamma - \langle E_\gamma \rangle)^2 \rangle = & \frac{-\lambda_1}{12} + M_B^2 (0.00815 \frac{\alpha_s}{\pi} + 0.01024 \beta_0 (\frac{\alpha_s}{\pi})^2) \\ & - \bar{\Lambda} M_B (0.05083 \frac{\alpha_s}{\pi} + 0.05412 \beta_0 (\frac{\alpha_s}{\pi})^2) - \frac{2\rho_1 - 3\rho_2}{12M_B} - \frac{\mathcal{T}_1 - 3\mathcal{T}_2}{12M_B} + \mathcal{O}(1/M_B^2). \end{aligned} \quad (3.2)$$

The  $1/M_B^3$  parameters  $\rho_i$ ,  $\mathcal{T}_i$  are estimated, from dimensional considerations, to be  $\sim (0.5\text{GeV})^3$ . Using Eq. 3.1,

$$\bar{\Lambda} = 0.35 \pm 0.08 \pm 0.10 \text{ GeV},$$

#### 4. $V_{cb}$ from hadronic mass moments

Using semileptonic decays the mass of the hadronic system  $X$  in  $B \rightarrow X_c \ell \nu$  is determined from the lepton and neutrino momentum vectors alone:

$$\begin{aligned} M_X^2 &= (E_B - E_\ell - E_\nu)^2 - (\vec{P}_B - \vec{P}_\ell - \vec{P}_\nu)^2 \\ &= M_B^2 + M_{\ell\nu}^2 - 2E_B E_{\ell\nu} + 2|\vec{P}_B||\vec{P}_{\ell\nu}| \cos \theta_{\ell\nu, B}. \end{aligned} \quad (4.1)$$

Because of the low momentum of the parent B  $M_X^2$  is approximated by

$$\widetilde{M}_X^2 = M_B^2 + M_{\ell\nu}^2 - 2E_B E_{\ell\nu}. \quad (4.2)$$

The background-subtracted  $\widetilde{M}_X^2$  distribution, consisting of 11900  $B$  meson decays, is shown in Figure 5. For the purpose of extracting the moments of the  $M_X^2$  distribution, the  $b \rightarrow c \ell \nu$  decays is divided into three components:  $B \rightarrow D \ell \nu$ ,  $B \rightarrow D^* \ell \nu$ , and  $B \rightarrow X_H \ell \nu$  where  $X_H$  represents all the high mass charmed meson resonances as well as the charmed non-resonant decays. The individual components are shown in Figure 5. We use measured form factors [12] to model the  $B \rightarrow D \ell \nu$  and  $B \rightarrow D^* \ell \nu$  decays. The  $M_X^2$  distributions for  $B \rightarrow D \ell \nu$  and  $B \rightarrow D^* \ell \nu$  which are broadened because of the incomplete reconstruction are generated by Monte Carlo. The high-mass contribution,  $B \rightarrow X_H \ell \nu$ , is modeled using six resonances of the  $D^{**}$  and non resonant multi particle decays.

A fit of the Monte Carlo to the data  $\widetilde{M}_X^2$  distribution determines the relative contributions from  $B \rightarrow D \ell \nu$ ,  $B \rightarrow D^* \ell \nu$  and  $B \rightarrow X_H \ell \nu$ . The relative rates and the generated masses are used to calculate  $\langle M_X^2 - \bar{M}_D^2 \rangle$  and  $\langle (M_X^2 - \bar{M}_D^2)^2 \rangle$  of the true  $M_X^2$  distribution. Equation 4.3 shows the derivation of the average mass squared,  $M_X^2$ , from the relative rates.

$$\langle M_X^2 \rangle = r_D \cdot M_D^2 + r_{D^*} \cdot M_{D^*}^2 + r_{X_H} \cdot \langle M_{X_H}^2 \rangle, \quad (4.3)$$

where  $r_D$  is the rate of  $B \rightarrow D \ell \nu$  production compared to the combined rate of  $B \rightarrow D \ell \nu$ ,  $B \rightarrow D^* \ell \nu$ ,  $B \rightarrow X_H \ell \nu$ , and similarly for  $r_{D^*}$  and  $r_{X_H}$ . The individual values obtained for

$r_D$ ,  $r_{D^*}$  and  $r_{X_H}$ , while perfectly consistent with world average branching fractions [14], are not well determined and are sensitive to the model chosen for  $B \rightarrow X_H \ell \nu$ . The *moments*, however, are well-determined and stable against model changes, as discussed below. The analysis yields  $\langle M_X^2 - \bar{M}_D^2 \rangle \equiv M1 = 0.251 \pm 0.023 \pm 0.062 \text{ GeV}^2$ ,  $\langle (M_X^2 - \bar{M}_D^2)^2 \rangle \equiv M2 = 0.639 \pm 0.056 \pm 0.178 \text{ GeV}^4$ , and  $\langle (M_X^2 - \langle M_X^2 \rangle)^2 \rangle \equiv M2' = 0.576 \pm 0.048 \pm 0.163 \text{ GeV}^4$ , where the errors are statistical and systematic, in that order. The experimental errors on  $\langle (M_X^2 - \langle M_X^2 \rangle)^2 \rangle$  are somewhat smaller than for  $\langle (M_X^2 - \bar{M}_D^2)^2 \rangle$  and have a smaller correlation with the first moment. (A correction for final state radiation, not included in the Monte Carlo samples used in our fits, has been applied, using PHOTOS [13].)

The expressions [10, 15] for the hadronic mass moments in  $B \rightarrow X_c \ell \nu$ , to order  $\beta_0 \alpha_s^2$  and  $1/M_B^3$ , subject to the restriction  $P_\ell > 1.5 \text{ GeV}/c$ , are given in Eqs. 4.4 and 4.5. (Due to technical difficulties, the coefficients of the  $\frac{\bar{\Lambda}}{M_B} \frac{\alpha_s}{\pi}$  terms were computed *without* the 1.5 GeV lepton energy restriction, and so are only approximate, believed good to  $\pm 50\%$ .)

$$\begin{aligned} \frac{\langle M_X^2 - \bar{M}_D^2 \rangle}{\bar{M}_B^2} = & [0.0272 \frac{\alpha_s}{\pi} + 0.058 \beta_0 \frac{\alpha_s^2}{\pi^2} + 0.207 \frac{\bar{\Lambda}}{M_B} (1 + 0.43 \frac{\alpha_s}{\pi}) + 0.193 \frac{\bar{\Lambda}^2}{M_B^2} + 1.38 \frac{\lambda_1}{M_B^2} + 0.203 \frac{\lambda_2}{M_B^2} \\ & + 0.19 \frac{\bar{\Lambda}^3}{M_B^3} + 3.2 \frac{\bar{\Lambda} \lambda_1}{M_B^3} + 1.4 \frac{\bar{\Lambda} \lambda_2}{M_B^3} \\ & + 4.3 \frac{\rho_1}{M_B^3} - 0.56 \frac{\rho_2}{M_B^3} + 2.0 \frac{\mathcal{T}_1}{M_B^3} + 1.8 \frac{\mathcal{T}_2}{M_B^3} + 1.7 \frac{\mathcal{T}_3}{M_B^3} + 0.91 \frac{\mathcal{T}_4}{M_B^3} + \mathcal{O}(1/\bar{M}_B^4)], \quad (4.4) \end{aligned}$$

$$\begin{aligned} \frac{\langle (M_X^2 - \langle M_X^2 \rangle)^2 \rangle}{M_B^4} = & [0.00148 \frac{\alpha_s}{\pi} + 0.0025 \beta_0 \frac{\alpha_s^2}{\pi^2} + 0.027 \frac{\bar{\Lambda}}{M_B} \frac{\alpha_s}{\pi} + 0.0107 \frac{\bar{\Lambda}^2}{M_B^2} - 0.12 \frac{\lambda_1}{M_B^2} \\ & + 0.02 \frac{\bar{\Lambda}^3}{M_B^3} - 0.06 \frac{\bar{\Lambda} \lambda_1}{M_B^3} - 0.129 \frac{\bar{\Lambda} \lambda_2}{M_B^3} \\ & - 1.2 \frac{\rho_1}{M_B^3} + 0.23 \frac{\rho_2}{M_B^3} - 0.12 \frac{\mathcal{T}_1}{M_B^3} - 0.36 \frac{\mathcal{T}_2}{M_B^3} + \mathcal{O}(1/\bar{M}_B^4)] \quad (4.5) \end{aligned}$$

In these expressions,  $\bar{M}_B$  represents the spin-averaged  $B$  meson mass, 5.313 GeV.

The  $1/M_B^3$  parameters  $\rho_i$ ,  $\mathcal{T}_i$  are estimated [11], from dimensional considerations, to be  $\sim (0.5 \text{ GeV})^3$ . Taking values of  $\rho_2$  and  $\mathcal{T}_1$  through  $\mathcal{T}_4$  to be  $0.0 \pm (0.5 \text{ GeV})^3$ , taking  $\rho_1$  (believed to be positive) to be  $\frac{1}{2}(0.5 \text{ GeV})^3 \pm \frac{1}{2}(0.5 \text{ GeV})^3$ , and taking  $\lambda_2 = 0.128 \pm 0.010 \text{ GeV}^2$  (appropriate with a calculation to order  $1/M_B^3$ ), the expressions combined with our measurements define bands in  $\bar{\Lambda} - \lambda_1$  space. The band for the first moment is shown in Figure 6. The dark grey region indicates the error band from the measurement; the light grey extension includes the error from the theoretical expression, in particular from the  $\rho_1 - \mathcal{T}_4$  terms and from the scale uncertainty ( $\alpha_s(m_b/2)$  to  $\alpha_s(2m_b)$ ).

Also included is the band defined by the  $b \rightarrow s \gamma$  analysis. The intersection of the two bands from the first moments determines  $\bar{\Lambda}$  and  $\lambda_1$ . A  $\Delta\chi^2 = 1$  ellipse is shown. The values obtained are

$$\bar{\Lambda} = 0.35 \pm 0.07 \pm 0.10 \text{ GeV} ,$$

$$\lambda_1 = -0.238 \pm 0.071 \pm 0.078 \text{ GeV}^2 .$$

Here, the first error is from the experimental error on the determination of the two moments, and the second error from the theoretical expressions. (Using the information from all four bands, first and second moments, the results differ little, both as to central values and as to errors.) Note that  $\bar{\Lambda}$  and  $\lambda_1$  are scheme and order dependent. The values obtained above are for  $\bar{\Lambda}$  and  $\lambda_1$  to order  $1/M^3$ , order  $\beta_0\alpha_s^2$ , in the  $\overline{MS}$  renormalization scheme.

Using these results  $|V_{cb}|$  can now be determined from the measured  $B \rightarrow X_c \ell \nu$  semileptonic width. The expression [16, 11] for the semileptonic width, to order  $\beta_0\alpha_s^2$  and  $1/M_B^3$ , is given in Eq. 4.6.

$$\begin{aligned} \Gamma_{sl} = \frac{G_F^2 |V_{cb}|^2 M_B^5}{192\pi^3} & 0.3689 \left[ 1 - 1.54 \frac{\alpha_s}{\pi} - 1.43 \beta_0 \frac{\alpha_s^2}{\pi^2} - 1.648 \frac{\bar{\Lambda}}{M_B} \left( 1 - 0.87 \frac{\alpha_s}{\pi} \right) - 0.946 \frac{\bar{\Lambda}^2}{M_B^2} - 3.185 \frac{\lambda_1}{M_B^2} \right. \\ & - 7.474 \frac{\lambda_2}{M_B^2} - 0.298 \frac{\bar{\Lambda}^3}{M_B^3} - 3.28 \frac{\bar{\Lambda}\lambda_1}{M_B^3} + 7.997 \frac{\bar{\Lambda}\lambda_2}{M_B^3} - 6.153 \frac{\rho_1}{M_B^3} + 7.482 \frac{\rho_2}{M_B^3} \\ & \left. - 7.4 \frac{\mathcal{T}_1}{M_B^3} + 1.491 \frac{\mathcal{T}_2}{M_B^3} - 10.41 \frac{\mathcal{T}_3}{M_B^3} - 7.482 \frac{\mathcal{T}_4}{M_B^3} + \mathcal{O}(1/M_B^4) \right]. \end{aligned} \quad (4.6)$$

For the experimental determination of  $\Gamma_{sl}$ ,:  $\mathcal{B}(B \rightarrow X_c \ell \nu) = (10.39 \pm 0.46)\%$  [17],  $\tau_{B^\pm} = (1.548 \pm 0.032)$  ps [14],  $\tau_{B^0} = (1.653 \pm 0.028)$  ps [14],  $f_{+-}/f_{00} = 1.04 \pm 0.08$  [18], giving  $\Gamma_{sl} = (0.427 \pm 0.020) \times 10^{-10}$  MeV.

Combining the measured semileptonic width with the theoretical expression, and using the determination of  $\bar{\Lambda}$  and  $\lambda_1$  from the first moments,

$$|V_{cb}| = (4.04 \pm 0.09 \pm 0.05 \pm 0.08) \times 10^{-2},$$

where the errors are from experimental determination of  $\Gamma_{sl}$ , from experimental determination of  $\bar{\Lambda}$  and  $\lambda_1$ , and from the  $1/M_B^3$  terms and scale uncertainty in  $\alpha_s$ , in that order. This gives a determination of  $|V_{cb}|$  from inclusive processes, with a precision of  $\pm 3.2\%$ . This result depends on the assumption of global parton-hadron duality, and with it unknown uncertainties.

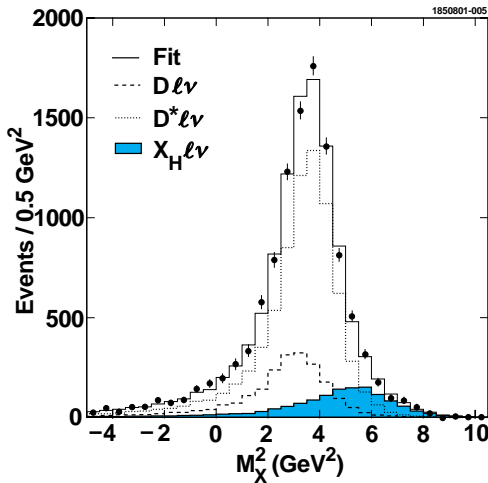


**Figure 5:** Measured  $\widetilde{M}_X^2$  distributions, for background corrected data (points), and the three components of the Monte Carlo.

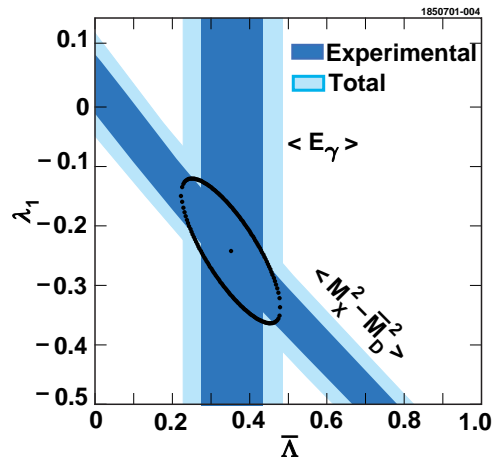


**Figure 6:** Bands in  $\bar{\Lambda} - \lambda_1$  space defined by  $\langle M_X^2 - \bar{M}_D^2 \rangle$  and  $\langle E_\gamma \rangle$ .

## References

- [1] R. Barlow and C. Beeston, *Comp. Phys. Comm.* **77**, 219 (1993).
- [2] I. Caprini, L. Lellouch and M. Neubert, *Nucl. Phys.* **B 530**, 153 (1998) [hep-ph/9712417].
- [3] C. G. Boyd, B. Grinstein, R. F. Lebed, *Phys. Rev. D* **56**, 6895 (1997) [hep-ph/9705252].
- [4] J. Duboscq *et al.*, CLEO Collaboration, *Phys. Rev. Lett.* **76**, 3898 (1996).
- [5] M. Neubert, *Physics Reports*, **245**, 259 (1994).
- [6] A. L. Kagan and M. Neubert, *Eur. Phys. J.* **C 7**, 5 (1999).
- [7] Z. Ligeti, M. Luke, A. V. Manohar, and M. B. Wise, *Phys. Rev. D* **60** 034019, (1999); C. Bauer, *Phys. Rev. D* **57**, 5611. (1998).
- [8] Adam Falk and Zoltan Ligeti, private communications.
- [9] M. Neubert, hep-ph/9809377.
- [10] A. Falk, M. Luke, and M. Savage, *Phys. Rev. D* **53**, 2491 (1996); *ibid*, **53**, 6316 (1996).
- [11] M. Gremm and A. Kapustin, *Phys. Rev. D* **55**, 6924 (1997).
- [12] J. Bartelt *et al.* (CLEO), *Phys. Rev. Lett.* **82**, 3746 (1999); J. Duboscq *et al.* (CLEO), *Phys. Rev. Lett.* **76**, 3898 (1996).
- [13] E. Barberio and Z. Wąs, *Comput. Phys. Commun.* **79**, 291 (1994).
- [14] D. E. Groom *et al.* (PDG) *Eur. Phys. J.* **C 15**, 1 (2000).
- [15] A. Falk and M. Luke, *Phys. Rev. D* **57**, 424 (1998).
- [16] I. I. Bigi, N. G. Uraltsev, and A. I. Vainshtein, *Phys. Lett.* **B 293**, 430 (1992); Erratum, *Phys. Lett.* **B 297**, 477 (1993); M. Jezabek and J. H. Kühn, *Nucl. Phys. B* **314**, 1 (1989); M. Luke, M. J. Savage, and M. B. Wise; *Phys. Lett.* **B 345**, 301 (1995).
- [17] B. Barish *et al.* (CLEO), *Phys. Rev. Lett.* **76**, 1570 (1996). (We reduce the semileptonic branching fraction by 1% of itself, to correct for the  $b \rightarrow u\ell\nu$  contribution.)
- [18] J. P. Alexander *et al.* (CLEO), *Phys. Rev. Lett.* **86**, 2737 (2001).